Supporting Information

Jenny et al. 10.1073/pnas.1605480113

SI Materials and Methods

Paleolimnological Data. A literature search was conducted in April 2014 (17) and updated in June 2015 using the Institute for Scientific Information Web of Science database and Google Scholar with different combinations of the following keywords: "varve" and "lake," and "lamin" and "lake sediment." The search yielded 148 relevant European lakes that contain laminated or varved sediments. Descriptions and data on varved sites, sediments, and dating methods are available in a study by Jenny et al. (ref. 17 and the references therein). The original chronologies were expressed in CE calendar years. Laminated lacustrine sites had to satisfy several conditions to be included in this synthesis. Accepted sites contained a varved or well-preserved laminated sedimentary sequence and/or featured a published age-model relying on varve counting and/or radiometric dating, and the lakes' sediment texture had to be explicitly described or illustrated by pictures outlining the laminated intervals. The timing of the first onset of hypoxia was obtained for each lake by examining all relevant published varve data. Where time intervals could not be dated precisely with the help of published data, corresponding authors were contacted and asked for advice. The water depth for each lake was collected and used to verify that lake level fluctuations were not the cause of changes in preservation conditions of the varves. Descriptions and data for lake sites were compiled in this study (Table S1).

Land Use and Climate Data. Modern data and temporal changes in land use and climate during the past 300 years were analyzed for 1,607 watersheds. Hydrological basins of each site were calculated using the flow accumulation and flow direction rasters made available from hydrological data and maps based on Shuttle Elevation Derivatives at Multiple Scales (HydroSHEDS), together with lake perimeters and areas using the GLWD from the World Wildlife Foundation (38). The following variables were extracted from modeled areas using the "Arc" geographic information system (ArcGIS): (*i*) modern site characteristics, (*ii*) past land use from CE 1900–2010 at decadal steps and with a 1-km^2 spatial resolution, and (*iii*) past land use from CE 1700–2000 with centennial resolution. Mean local temperatures; precipitations; population densities (65); changes in urban cultivated, pastured, and forest areas (24); and past human population densities (66) were extracted from modeled areas for each watershed.

Multiple regression analyses were conducted to identify the main drivers of hypoxia onsets. For each recently hypoxic lake ($n = 51$), we created a binomial time series indicating whether the first hypoxic event had occurred or not at each date of the land cover data (i.e., CE 1700, 1800, 1900, 1910, . . ., 2010). To test the relative importance of the different land cover types, we then ran a logistic GAMM using the binomial time series as the response variable; the percentage of urban, cultivated, and pastured areas as fixed effect explanatory variables; and lake identification as the random effect (testing a random slope and intercept for each lake). To test further whether the smooth term varied among lakes, we tested a random smooth logistic GAMM, which allowed not only the slope to vary among lakes but also the shape of the nonlinear relationship. All GAMMs were fit using the bam function of the itsadug package in R (67).

Nonparametric M-K tests for monotonic trends were used to quantify trends of land use for each of the 1,607 watershed time series within the past 300 years. This analysis was based on the Kendall rank correlation coefficient and was conducted using the Kendall library (68). A positive score shows a monotonically increasing trend, whereas a negative value shows a monotonically decreasing trend (69). For each site, M-K tests were run for two time windows to identify the potential effects of slow and fast land cover changes on the hypoxia onset: We anticipated that fast changes in the land cover would show an effect within a short period (±20 years) centered on the time of the onset to be consistent with the uncertainties of reconstructions, and that slow changes in the land cover would show an effect over a longer period (~200 years) preceding the onset of hypoxia to be consistent with the long-term history and potential legacy effects of past land changes in Europe.

SI Text

Specific details on selected sites are described in Fig. S6 and Table S2.

Lakes Geneva (Léman), Bourget, and Annecy are located in the French and Swiss perialpine region and were intensively studied in the course of the program: Perturbation Impacts on Lake Food Webs, a Palaeo-Ecological Approach (IPERRETRO) of the French National Research Agency (ANR) (2009–2013) (12, 35). Within this program, volumes of hypoxic waters were reconstructed and analyzed during the Anthropocene using limnological and paleolimnological data (35, 46). The three lakes were selected because they share the same P enrichment history: although they were oligotrophic at the end of the 19th century, all three lakes underwent P enrichment as early as the 1920s, concomitant to the population increase in urban areas (Fig. S6). At this time, these lakes received untreated wastewaters from the growing cities of Geneva, Chambéry, Aix-Les-Bains, and Annecy (Fig. S6). A shift to hypoxic conditions occurred in CE 1933 ± 1, CE 1950 ± 1, and CE 1952 ± 1 [in Bourget, Geneva (Léman) and Annecy, respectively] in response to the unprecedented rise in total P concentrations above 10 ± 5 μg of P L^{-1}. Following this shift, hypoxia never disappeared, despite the fact that the environmental policies implemented succeeded in drastically reducing lake P concentrations: Observational data demonstrate that mean total phosphorus (TP) values measured during winter mixing have been successfully reduced to 6 μg of P L^{-1} in Annecy, 19 μg of P L^{-1} in Geneva, and 17 μg of P L^{-1} in Bourget (47).

Lake Alserio, a dimictic hard-water eutrophic lake, is located in the Brianza district near Lake Como in northern Italy (surface area of 1.23 km^2 and maximum depth of 5.3 m). Beginning in the 1970s, Lake Alserio was affected by elevated external P loads, which resulted in high P concentrations in the water column (73). The major P sources that affected the water quality and the trophic status of the lake were domestic sewage (fluxes of P to the sediments = 1.96 $g \cdot m^{-2} \cdot a^{-1}$) and runoff (fluxes of P to the sediments = 0.75 $g \cdot m^{-2} \cdot a^{-1}$) (73). Despite both the reduction of P in detergents and the construction of a pipe conveying urban wastewater and runoff to a treatment plant, the present external P load to the lake is still high. The change from homogeneous sediment to a laminated sequence appears to be linked to the eutrophication process of Lake Alserio occurring since the 1960s (73).

Baldeggersee is located on the central Swiss Plateau, and is characterized by a maximum depth of 66 m, a surface area of 5.2 km^2, and a water renewal time of 5.6 years. Owing to strong anthropogenically driven nutrient enrichment of this site, Baldeggersee has become hypertrophic, and complete oxygen depletion was observed at water depths of 60 m at the beginning of this century (55). Long-term changes in the watershed showed that growing urbanization was concomitant with the onset of hypoxia in 1880s (as inferred from the lake sediment record). The introduction of treatment plants since 1967 and 1975 has successfully reduced point sources of nutrients (55). Since 1982, bioturbation has prevented varve formation above 55 m of water depth due to the better oxygen regimes at the water/sediment interface. However, below 55 m in water depth, the mineralization of organic carbon is still causing oxygen depletion that allows the formation and preservation of varves.

Lake Jyväsjärvi is located in central Finland (64°14′N, 25°47′E) and has a surface area of 3.4 km^2 and a maximum depth of 27 m. The town of Jyväskylä was established on the lakeshore in 1837 on the northern bank of Lake Jyväsjärvi, and the lake received untreated municipal wastewater from the town up until 1977 (74). Based on the biological and chemical properties of the sediment strata, Meriläinen et al. (74) distinguished a phase of early changes in the lake ecosystem from the 1870s to *ca.* the 1940s. This phase of early changes corresponds well to the timing when varves first appeared (at the end of the 1800s) and when the lake received untreated municipal wastewater. Although the first plans for building a wastewater treatment plant were prepared in the early 1930s, municipal wastewater continued to be discharged into the lake in the untreated form until 1977. In recent years, this effluent loading has been reduced.

With a surface of 61.8 km^2 and a volume of 7.5 km^3, Lake Iseo (also known as Sebino) is the fourth largest Italian lake. The watershed includes 83 municipalities, 21 of which are on the shoreline, with a total population of about 180,000 inhabitants. The sources of P in Lake Iseo are derived mainly from point sources (75). During the 1960s, intensifying eutrophication processes and the corresponding deterioration of water quality in northern Italy were becoming apparent, initially in lakes with low maximum depths (Lake Varese and Lake Endine) and subsequently in the deep subalpine lakes. During the same period, Lake Iseo became hypoxic, as evidenced by the appearance of varved sediments.

Nylandssjön is located in northern Sweden (62°57′N, 18°17′E) and is a dimictic, mesotrophic, circumneutral lake. The lake is characterized by a surface area of 0.28 km^2 and a maximum depth of 17.5 m. The catchment (0.86 km^2) is covered mainly by spruce forest and, to a lesser extent, by arable land. Varves are evident in deeper sediment layers of Nylandssjön, but their permanent formation and preservation started at the beginning of the 20th century because of cultural eutrophication (76). The major population increase associated with wastewater release occurred at the end of the 19th century in the region of Lake Nylandssjön [there was a doubling in the number of inhabitants in the major town between CE 1850 and 1910 (Swedish population censuses, Statistikdatabasen), which has since stabilized].

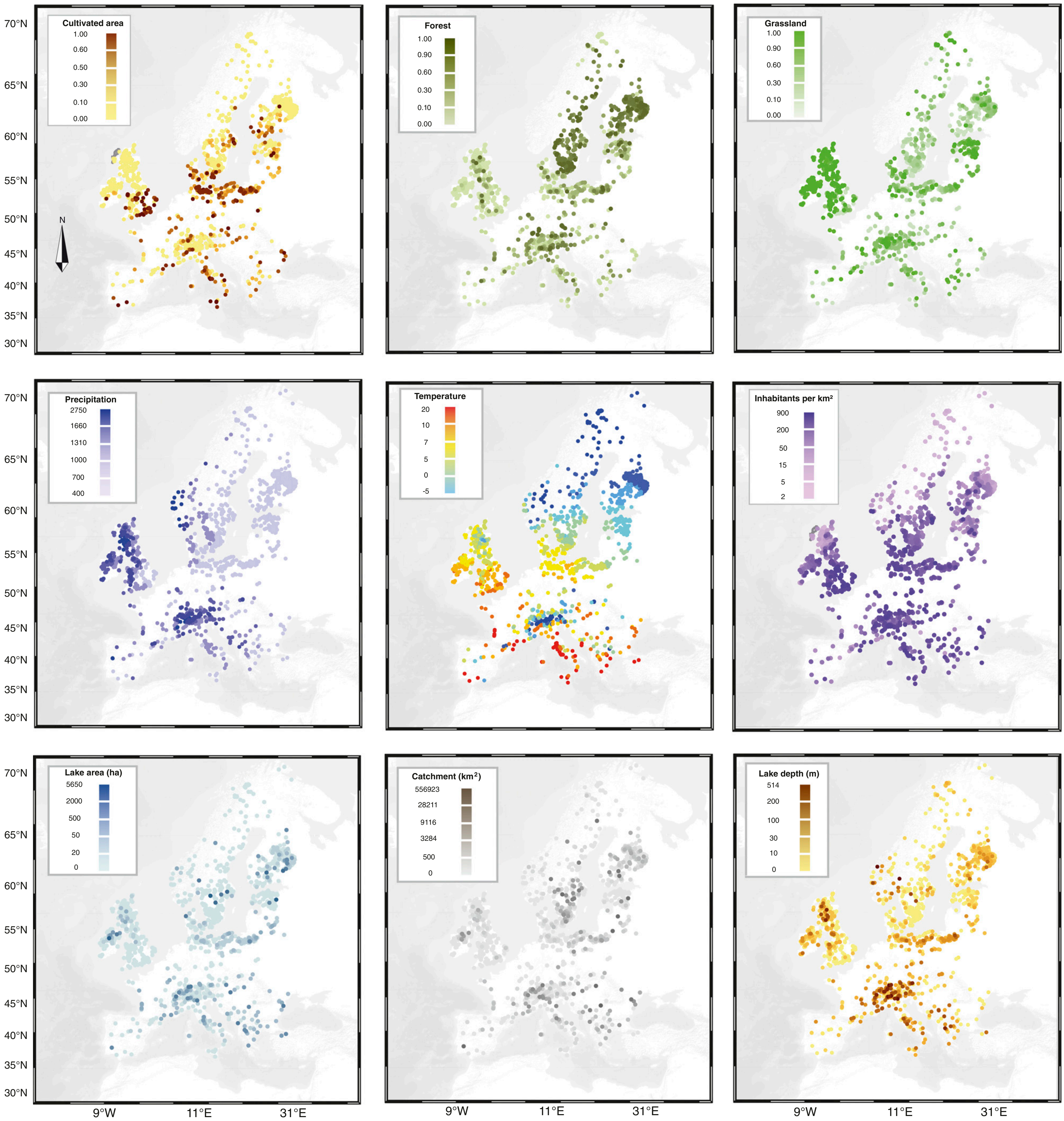

Fig. S1. Distribution of modern land cover, climate, and geomorphological properties in the studied European watersheds: cultivated area, forested area, pastured area, mean annual precipitation, mean annual air temperature, human population density, lake area, lake catchment size, and maximum lake water depth.

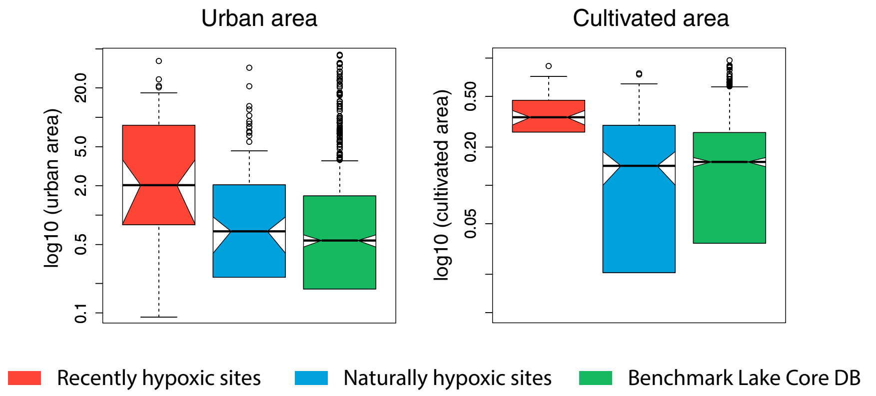

Fig. S2. Box plots describing the contemporary proportions of cultivated and urban areas in lake watersheds. Recently hypoxic sites (n = 51) are shown in red, naturally hypoxic sites (n = 97) are shown in blue, and benchmark watersheds (n = 769) are shown in green. Upper and lower population density limits represent the first and third quartiles.

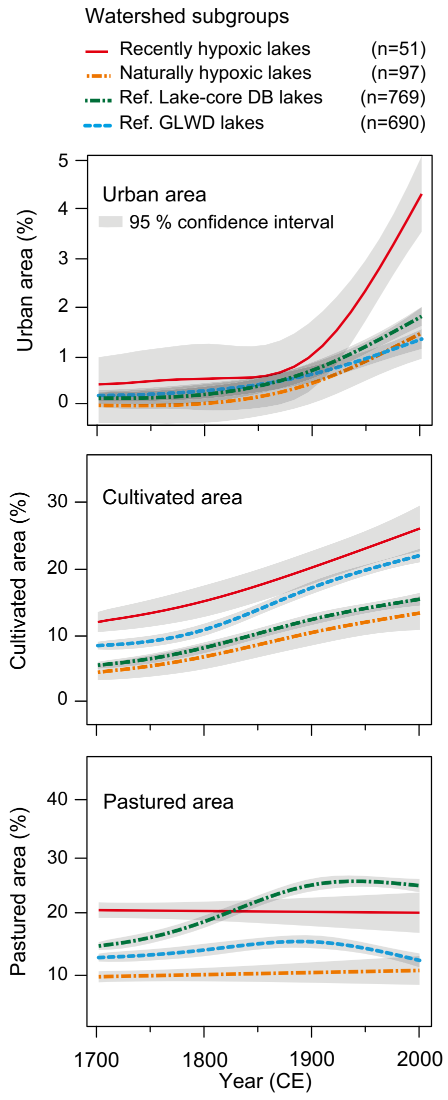

Fig. S3. Three hundred-year trends for land cover in Europe based on an AMM, grouping watersheds according to their history of downstream lake hypoxia or reference (Ref.) source. Land-cover values (63) were extracted from each modeled watershed (*Materials and Methods*). The increase in urban areas from CE 1700–2000 is significantly larger for watersheds with recently developed hypoxia (red solid line) than for watersheds with natural hypoxia (orange dashed line) and benchmark watersheds (green and blue dashed lines). All model results are statistically significant at $p < 0.0001$. Gray bands indicate 95% confidence intervals of the predicted means based on the AMM.

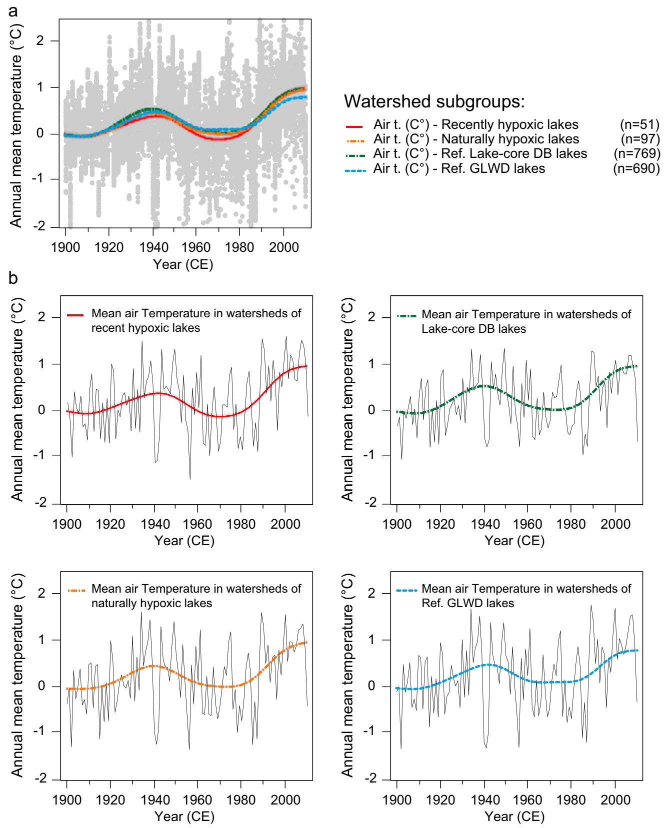

Fig. S4. Changes in air temperature (t.) during the past 110 years. (*A* and *B*) Mean annual temperatures are presented for all recently hypoxic sites, naturally hypoxic sites, and benchmark sites. Temperature anomalies have been extracted annually for each studied lake from the instrumental dataset of the University of Delaware Air Temperature & Precipitation (UDEL) model (global data with a resolution of 0.5° × 0.5°). Color lines are fifth-order polynomial trends, and gray lines are 95% confidence intervals. (*A*) Trends for each subgroup of lakes have been superimposed. In CE 2000, there is no significant difference in temperature anomalies between recently hypoxic sites, naturally hypoxic sites, and benchmark sites. DB, database.

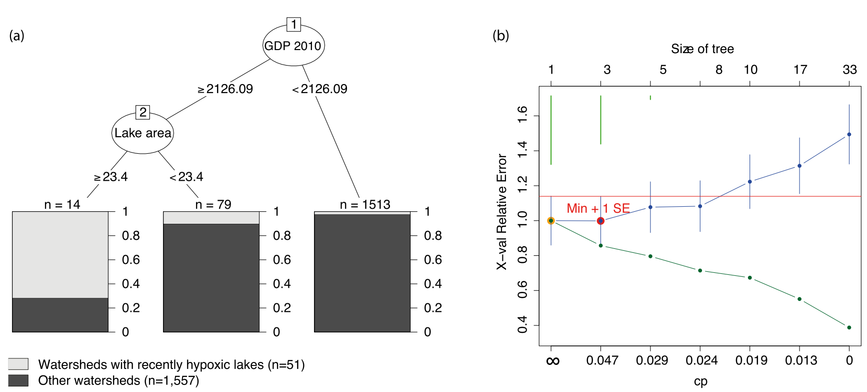

Fig. S5. (*A*) Regression tree of hypoxia onset for paleolimnological data. As a preliminary statistical assessment to describe the distribution of varves in European lakes, the modern land use and climate data for each watershed were used as the forcing variables and the presence/absence of varves in lake sediments was used as the response variable in a regression tree analysis using the *rpart* and the *wrapper* function "MVPARTwrap" (69) in R, v3.0.2 (R Foundation for Statistical Computing). Plots of the cross-validation results and pruning of the tree using the 1-SE rule (69) were used to select the best tree and to avoid overfitting. (*B*) Specifically, we chose the complexity parameter associated with the smallest tree where the estimated error rate was within 1 SE of the minimum error, and pruned the tree at this complexity parameter value. Several cross-validation runs were performed to verify that the final tree was not atypical. We compiled data for numerous potential explanatory variables that have previously been shown to explain significant variation in hypoxia distribution. In particular, the variables considered for the regression tree analysis included modern data on lakes, land use, climate, and human activities, as described in *Materials and Methods*, *Land Use and Climate Data*. The distribution of hypoxic lakes was also compared with human population density and with gross domestic product (GDP), serving as a potential factor affecting the P yields to lakes. We used a conservative variation inflation factor (VIF < 5) to isolate independent (noncollinear) explanatory variables and eliminated collinear variables to improve interpretation of the regression trees. Explanatory variables retained for the final regression tree included maximum lake depth, urban area, forest area, pastured area, lake surface area, precipitation, air temperature, human population, GDP, and maximum depth. cp, complexity parameter.

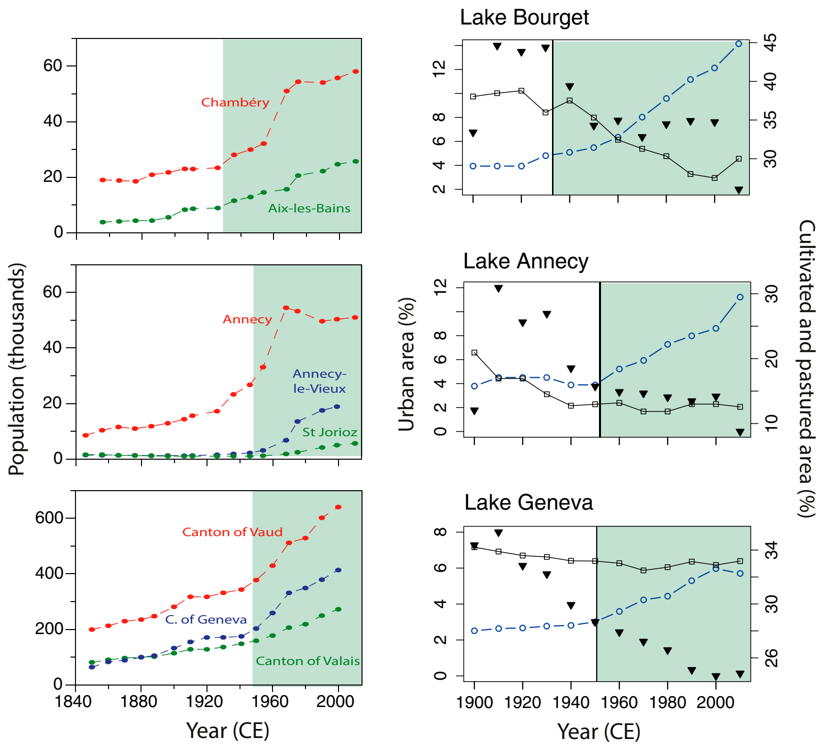

Fig. S6. Specific details on perialpine Lakes Geneva (Leman), Bourget, and Annecy. Changes in land cover (*Right*) and human population (*Left*) are presented for the three sites. (*Right*) Percentages of urban (blue curves with circles), cultivated (black curves with rectangles), and pastured (black triangles) areas are presented. Periods with the hypoxic condition in lakes are highlighted in green. Urban area and population are growing at the time of the hypoxia onset, whereas cultivated and pastured areas are decreasing.

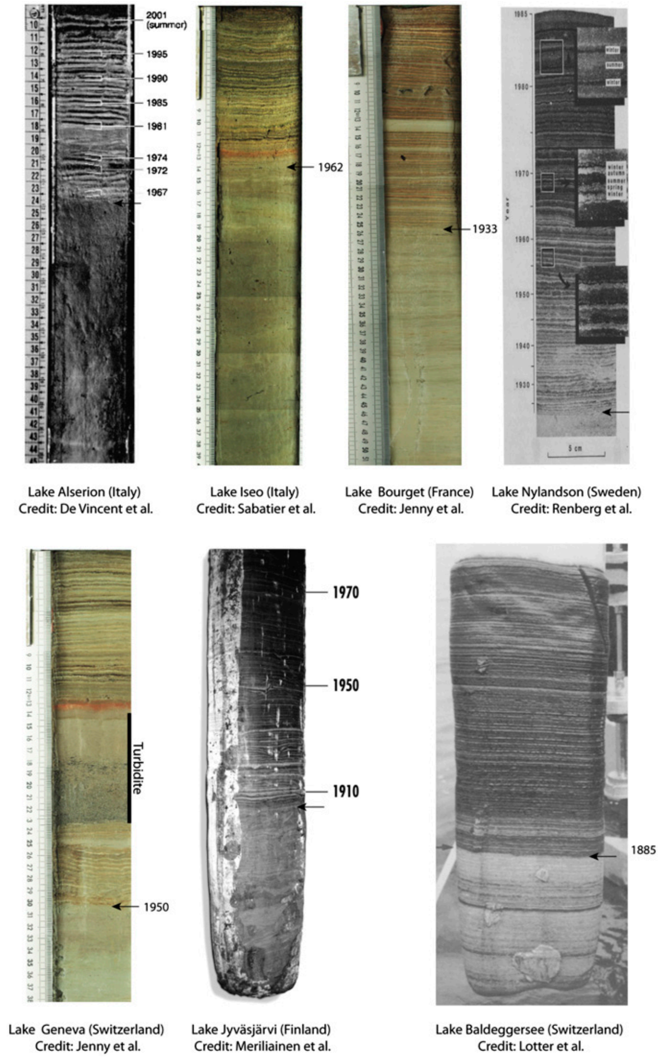

Fig. S7. Examples of hypoxia onset in a subset of lake sediment cores used in this study, illustrating the appearance of laminated sediment on top of homogeneous sediment. The appearance of these sedimentary facies indicates that annual oxygenation conditions fell below a critical threshold in both duration and concentration, hence recording the die-out of macrobenthos and the end of its related bioturbation. Specific details on those individual sites across Europe are presented in *SI Text* [De Vincent et al. (73); Jenny et al. (46); Renberg et al. (76); Jenny et al. (35); Merilianan et al. (74); Lotter et al. (55)].

Table S1. Descriptive statistics of lake and catchment properties

	Recently hypoxic lakes (n = 51)			Naturally hypoxic lakes (n = 97)			Benchmark, Lake Core Database (n = 769)			Benchmark, GLWD (n = 690)		
Parameters	Mean	Min.	Max.	Mean	Min.	Max.	Mean	Min.	Max.	Mean	Min.	Max.
Altitude, m	511	25	2,445	494	21	2,826	438	0	3,028	317	1	2,550
Lake area, ha	60	0	582	7	0	290	25	0	5,650	21	0	1,856
Maximum depth, m	62	2	310	28	0	410	14	0	449	24	0	514
Catchment, km^2	1,620	0	25,972	524	0	22,523	253	0	47,375	1,725	0	556,923
Precipitation, $mm \cdot a^{-1}$	821	471	1,577	819	406	2,002	1,022	458	2,755	742	420	1,853
Urban area, %	8	0	100	5	0	100	3	0	100	2	0	98
Cultivated area, %	12	0	100	9	0	100	10	0	100	15	0	100
Forested area, %	38	0	99	52	0	100	34	0	100	50	0	100
Pastured area, %	27	0	82	24	0	100	42	0	100	20	0	100
Other land, %	6	0	100	7	0	100	8	0	100	2	0	97
Inhabitant per km^2	183	0	1,530	77	0	1,504	108	0	8,537	69	1	3,527

Mean, minimum (Min.), and maximum (Max.) are reported for the four lake categories of this study: recently hypoxic lakes, naturally hypoxic lakes, and two sets of benchmark lakes. Air temperatures are mean annual anomalies (°C).

Table S2. Inventory of sites recording the onset of hypoxia

Site	Country	Latitude, DD	Longitude, DD	Facies top section	Hypoxia onset date, CE	Altitude, m	Lake area, km^2	Catchment area, km^2	Maximum depth, m	Source	DOI
Alserio	Italy	45.78703	9.21512	Varves	1967	260	1.23	18.3	8.1	(73)	10.1007/s10933-005-6786-2
Ammersee	Germany	48.06470	11.12416	Varves	1958	533	46.60	993.0	81.1	(77)	10.1029/2009WR008360
Annecy	France	45.89803	6.13572	Varves	1952	447	27.60	251.0	41.5	(35)	10.1002/2014GB004932
Arendsee	Germany	52.89035	11.47772	Varves	1965	22.8	5.14	29.8	48.7	(78)	10.1016/S0031-0182(01)00403-5
Baldeggersee	Switzerland	47.19777	8.26249	Varves	1885	463	5.22	68.4	66.0	(55)	10.1007/BF02522361
Białoławki	Poland	53.73538	21.82862	Laminated	1971	116	2.11	12.7	36.1	(58)	10.1007/s10933-013-9741-7
Blelham Tarn	England	54.39593	−2.97734	Laminated	1980	44	0.11	4.3	14.5	(79)	10.1023/A:1024437426878
Bourget	France	45.80111	5.82652	Varves	1933	231	44.50	560.0	145.0	(46)	10.4319/lo.2013.58.4.1395
Bussjösjön	Sweden	55.44559	13.80172	Laminated	1900	40	0.03	0.5	3.0	(80)	10.1023/A:1007967832177
Constance	Germany	47.65811	9.28918	Varves	1890	395	571.50	11,477.0	254.0	(81)	10.1007/BF02538288
Dgał Mały	Poland	54.12157	21.78924	Laminated	1972	120	0.94	33.0	16.8	(58)	10.1007/s10933-013-9741-7
Enonselka Vesijarvi	Finland	61.01707	25.60596	Varves	1960	81	26.00	84.0	33.0	(82)	10.1007/978-94-017-3622-0_42
Frickenhauser See	Germany	50.40286	10.23707	Varves	1870	315	0.11	0.1	14.5	(83)	10.1177/0959683607086762
Gallocanta	Spain	40.97208	−1.50390	Laminated	1960	990	14.14	543.0	2.5	(84)	10.1016/S0037-0738(01)00217-2
Garbas	Poland	53.90390	22.16229	Laminated	1968	129	0.42	8.0	38.0	(58)	10.1007/s10933-013-9741-7
Geneva	Switzerland	46.21825	6.16220	Varves	1950	372	582.00	7,975.0	310.0	(35)	10.1002/2014GB004932
Gennarbyviken	Finland	60.02937	23.31161	Varves	1957	41	10.77	88.2	32.0	(85)	10.1007/978-94-009-7290-2_24
Greifensee	Switzerland	47.35885	8.669117	Varves	1916	435	24.00	147.8	32.0	(86)	10.1023/B:HYDR.0000014038.64403.4d
Iseo	Italy	45.67459	10.05160	Varves	1962	186	60.90	1,736.0	251.0	(87)	10.1016/j.chemosphere.2011.06.037
Jaczno	Poland	54.28322	22.87151	Laminated	1963	163	0.41	9.0	29.6	(58)	10.1007/s10933-013-9741-7
Jyväsjärvi	Finland	62.23918	25.77259	Varves	1905	78	3.40	372.0	27.0	(74)	10.1023/B:JOPL.0000007229.46166.59
Kameduł	Poland	54.26666	22.86666	Laminated	1968	160	0.25	10.8	24.5	(58)	10.1007/s10933-013-9741-7
Kocioł	Poland	53.72016	21.85844	Laminated	1988	116	2.90	27.7	26.4	(58)	10.1007/s10933-013-9741-7
Kolje	Poland	54.27964	22.88721	Laminated	1968	149	0.16	3.8	27.5	(58)	10.1007/s10933-013-9741-7
Kuokkajarvi	Finland	61.68806	30.62095	Laminated	1825	21	2.55	28.5	19.0	(88)	10.1007/s10933-005-2542-x
Lago Albano	Italy	41.74656	12.67117	Varves	1948	293	6.00	3.7	175.0	(89)	10.1007/BF00684032
Lago Grande di Avigliana	Italy	45.06648	7.38725	Varves	1935	353	0.83	10.7	26.0	(90)	10.1007/s10933-006-0002-x
Laitialanselka Vesijärvi	Finland	61.07889	25.40059	Varves	1970	81	21.50	159.0	18.0	(82)	10.1007/978-94-017-3622-0_42
Lavijarvi	Finland	68.52848	22.60507	Varves	1935	6	2.01	74.0	22.0	(88)	10.1007/s10933-005-2542-x
Ławki	Poland	53.91050	21.57785	Laminated	1992	117	0.69	6.8	17.0	(58)	10.1007/s10933-013-9741-7
Lemiet	Poland	54.15833	21.81333	Laminated	1981	116	0.79	4.7	18.3	(58)	10.1007/s10933-013-9741-7
Lucerne Vitznau basin	Switzerland	47.01001	8.44979	Varves	1946	434	113.60	2,124.0	214.0	(91)	10.3406/rga.2003.2229
Lugano	Switzerland	45.98398	8.96945	Laminated	1929	271	48.70	565.0	288.0	(92)	10.1007/BF00878140
Neuchatel	Switzerland	46.94095	6.92148	Laminated	1952	429	215.00	2,672.0	153.0	(93)	10.1023/A:1008005622256
Nylandssjön	Sweden	62.94445	18.28138	Varves	1925	34	0.28	0.9	17.5	(94)	10.1111/j.1365-3091.2012.01343.x
Sacrower See	Germany	52.44589	13.10217	Varves	1873	29	1.07	35.3	38.0	(95)	10.1007/s10933-005-6188-5
San Puoto	Italy	41.28497	13.40856	Varves	1925	2	0.40	0.9	37.0	(96)	10.4081/jlimnol.2002.15
Sarkinen	Finland	64.13443	28.29127	Varves	1925	125	0.45	3.8	12.3	(97)	10.1007/BF00050950
Säynäjälampi	Finland	65.54768	29.62905	Varves	1960	300	263.00	17.9	1.5	(98)	10.1007/BF00028421
Sejwy	Poland	54.21166	23.18667	Laminated	1943	149	0.85	39.9	21.5	(58)	10.1007/s10933-013-9741-7
Siniec Maly	Poland	54.15124	21.51453	Laminated	1902	130	0.11	1.1	19.0	(58)	10.1007/s10933-013-9741-7

Table S2. Cont.

Site	Country	Latitude, DD	Longitude, DD	Facies top section	Hypoxia onset date, CE	Altitude, m	Lake area, km^2	Catchment area, km^2	Maximum depth, m	Source	DOI
St. Moritz	Switzerland	46.49405	9.845466	Varves	1910	1,768	0.78	171.0	44.0	(99)	10.1177/0959683607082555
Starnberger See	Germany	47.90414	11.30610	Varves	1939	584	56.40	315.0	120.0	(100)	10.1023/A:1008098118867
Tiefer Klocksin	Germany	53.59256	12.52857	Varves	1925	65	0.75	5.5	62.5	(101)	10.1007/s10933-013-9745-3
Tiefer Uckermark	Germany	53.23517	13.36204	Varves	1967	73	0.04	2.4	26.8	(101)	10.1007/s10933-013-9745-3
Tovel	Italy	46.26041	10.94891	Varves	1945	1,178	0.38	40.6	38.0	(89)	10.1007/BF00014627
Varese	Italy	45.81048	8.74287	Varves	1958	238	15.00	112.0	26.0	(102)	10.1007/978-94-009-4047-5_41
Vesijärvi	Finland	61.04159	25.58476	Varves	1912	81	110.00	515.0	42.0	(82)	10.1007/978-94-017-3622-0_42
Ziegelsee	Germany	53.65552	11.42552	Laminated	1996	38	3.00	11.0	34.4	(103)	10.1023/A:1022952232495
Zug	Switzerland	47.14571	8.48638	Varves	1850	417	38.00	204.0	201.0	(104)	10.1021/es950895t
Zurichsee	Switzerland	47.22266	8.75189	Varves	1895	406	88.00	1,829.0	143.0	(105)	10.1007/BF02538179

Watersheds for each lake were computed using the Shuttle Elevation Derivatives at Multiple Scales (HydroSHEDS) flow accumulation and flow direction rasters. Lake and sediment properties were compiled from published data: site country, coordinates in degree decimal, type of facies in the topmost section, age of hypoxia onset, altitude above sea level, lake area, catchment area, maximum depth, and the original reference and its DOI are shown. DD, decimal degrees.

Table S3. Land cover trends for recently hypoxic, naturally hypoxic, and benchmark sites

	Urban		Cultivated		Pastured		Total	
Hypoxicity	τ	*n*	τ	*n*	τ	*n*	*N*	Period
Recently hypoxic	+0.67	31	−0.29	40	−0.35	47	51	CE 1900–2010
Naturally hypoxic	+0.49	29	−0.18	52	−0.14	79	97	
Benchmark	+0.44	543	−0.14	674	−0.27	1,143	1,459	
Recently hypoxic	+0.92	24	+0.76	45	+0.22	45	51	CE 1700–2000
Naturally hypoxic	+0.91	31	+0.73	78	+0.42	72	97	
Benchmark	+0.91	558	+0.70	1,270	+0.55	1,245	14,59	

M-K test results are presented for recent (CE 1900–2010) and long-term (CE 1700–2000) periods. A positive score (red) indicates an increasing trend. Decreasing trends are shown in blue.

Table S4. Interaction between external drivers and lake hypoxia onset

	Sites recording increasing trends		Sites recording decreasing trends		Steady state	Total	
Area	%	*n*	%	*n*	*n*	*n*	Timing
Urban area	71	27	3	1	10	38	At the moment of hypoxia
Cultivated area	29	11	61	23	4	38	
Pastured area	21	8	74	28	2	38	
Urban area	43	19	0	0	25	44	Before hypoxia
Cultivated area	95	42	2	1	1	44	
Pastured area	80	35	20	9	0	44	

Increasing or decreasing trends in land cover are presented for two time windows: at the moment of hypoxia onset (±20 years centered on the moment of hypoxia onset) and before hypoxia onset (200 years preceding hypoxia onset). Numbers are color-coded to indicate when more than 40% of the sites showed an increase (red) or a decrease (blue) in urban, cultivated, or pastured area. The M-K tests presented in Fig. S3 confirm the increasing trends in urban area at the moment of hypoxia onset. Note that the urban area was generally increasing at the moment of hypoxia onset, whereas cultivated and pastured areas tended to be decreasing.